Manning free counterion fraction for a rodlike polyion: Aqueous solutions of short DNA fragments in presence of very low added salt

T. Vuletić,[1,*] S. Dolanski Babić,[1] D. Grgičin,[1] D. Aumiler,[1] J. Rädler,[2] F. Livolant,[3] and S. Tomić[1]

[1]*Institut za fiziku, 10000 Zagreb, Croatia*

[2]*Ludwig-Maximilians-Universität, Sektion Physik, Geschwister-Scholl-Platz 1, D-80539 Munich, Germany*

[3]*Laboratoire de Physique des Solides, Université Paris Sud, F-91405 Orsay, France*

(Received 27 December 2010; published 18 April 2011)

We quantified the Manning free (uncondensed) counterions fraction θ for dilute aqueous solutions of rodlike polyions: 150 bp DNA fragments, in the presence of a very low concentration of monovalent salt $c_{\text{salt}} < 0.05$ mM. Conductivity measurements of these solutions for DNA base pair concentration range $0.015 \leqslant c \leqslant 8$ mM were complemented by fluorescence correlation spectroscopy (FCS) measurements of the DNA polyion diffusion coefficient $D_p(c)$. We observed a crossover in the normalized conductivity $\sigma(c)/c$ that nearly halved across the $c = 0.05$–1 mM range, while $D_p(c)$ remained rather constant, as we established by FCS. Analyzing these data we extracted $\theta(c) = 0.30$–0.45, and taking the Manning asymmetry field effect on polyelectrolyte conductivity into account we got $\theta(c) = 0.40$–0.60. We relate the $\theta(c)$ variation to gradual DNA denaturation occurring, in the very low salt environment, with the decrease in DNA concentration itself. The extremes of the experimental $\theta(c)$ range occur toward the highest, above 1 mM, and the lowest, below 0.05 mM, DNA concentrations and correspond to the theoretical θ values for dsDNA and ssDNA, respectively. Therefore, we confirmed Manning condensation and conductivity models to be valuable in description of dilute solutions of rodlike polyions.

DOI: 10.1103/PhysRevE.83.041803 PACS number(s): 82.35.Rs, 87.15.hj, 66.30.hk

I. INTRODUCTION

Most biologically relevant macromolecules (DNA, proteins, polysaccharides) are polyelectrolytes with a very distinct behavior compared to neutral polymers or simple electrolytes [1,2]. When dissolved in polar solvents polyelectrolytes dissociate into a highly charged polyion (a macromolecule of extended shape) and many small counterions of low valency. The long-range nature of the electrostatic interactions and the entropy effects due to inhomogeneities in the counterion distributions and to a myriad of polyion configurations control their phenomenology.

The strong linear charge of the polyion tends to attract the counterions to its immediate vicinity. The condensation occurs for polyions with the Manning parameter $u = l_B/b > 1$, where l_B is the Bjerrum length, the length at which two elementary charges interact in a given solvent with energy equal to the thermal energy kT, and b is the average distance between the charges on the polyion backbone. If there is more than one charge per Bjerrum length, the condensation will tend to effectively reduce the linear charge density down to the $1/l_B$ level. The condensed ions fraction is then equal to $1 - 1/u$, and the free, uncondensed counterions fraction is $\theta = 1/u$. The condensation was modeled for an infinitely long and thin polyion in pure water, with no added salt, which might appear as a rather unrealistic proposition, with no biological relevance [3].

Counterion condensation is therefore more easily experimentally studied and the results theoretically interpreted for a dilute solution of rigid, monodisperse polyions, which do not change conformation with concentration. In a dilute solution, effectively, the condensed fraction of counterions may be considered to be found in a cylindrical cell around the polyion, while the rest may be taken to be free inside a larger volume that belongs to a given polyion [4]. According to the theory, since the condensed counterions are not chemically bound to the polyion, the free and condensed counterions exchange between the two concentric regions, and only a continuous radial counterion distribution [5] can exist around the polyion. In other words, there should be no step in the radial counterion distribution that would define the limit of the cylindrical zone, as shown experimentally by electron paramagnetic resonance [6].

Besides theoretical works considering two types of ions, experiments also attempt to quantify the condensed and free counterion fractions. Since only uncondensed, free counterions contribute to the osmotic pressure of a polyelectrolyte [7,8], the measured osmotic pressure of a polyelectrolyte solution evaluates the free counterions fraction [9–11]. The condensed counterions are those that move together with the polyion when an electric field is applied, while the free counterions would move in the opposite way due to their opposite charge [12–14]. Thus, the concept of two types of counterions gets a physical meaning.

Thus, the transport techniques may contribute to our knowledge of condensation in polyelectrolytes. The techniques range from electrical transport measurements like conductometry [12,15–17] and capillary electrophoresis [18,19] to diffusion measurements by dynamic light scattering [18–21] or fluorescence correlation spectroscopy [22,23]. Manning [24,25] has proposed a rather comprehensive and convincing conductivity model for polyelectrolytes, and Bordi *et al.* [14] worked on including the scaling theories by Rubinstein *et al.* [26], in order to separate the influences from the polyion (conformation and charges), the counterions, and the added salt.

For a successful quantitative study of Manning condensation by the transport experiments one has to use the simplest possible system: a dilute solution of monodisperse polyelectrolytes with no added salt. Also, an experimental method is needed to separate the influence of the charge

*http://tvuletic.ifs.hr/; tvuletic@ifs.hr

and conformation of the polyion on the (electrical) transport. Few experimental works met those requirements [9]. In other cases, there was a necessity to introduce the model for the conformation of the polyions into the interpretation of the conductivity data [12,15–17], which hinders the quantification of the Manning free counterions fraction.

Electrical conductivity in the system under study is a product of three separate factors characterizing the mobile charge carriers, summed over all charge species i in the system: their charge $z_i e$, their concentration n_i, and their mobility μ_i (ratio of carrier velocity and the applied electric field):

$$\sigma = \sum_i (|z_i|e) n_i \mu_i . \tag{1}$$

For simple electrolytes (see [12,14]), it is convenient to work with molar concentrations $c_i = n_i/N_A$ and equivalent conductivities $\lambda_i = F\mu_i$ (Faraday constant $F = eN_A$ and N_A is the Avogadro number). The conductivity is a sum of equivalent conductivities of the ionic species present in solution, multiplied by the charge (valence) z_i and concentration c_i of the respective ion:

$$\sigma = \sum_i z_i c_i \lambda_i . \tag{2}$$

For polyelectrolytes the expression of Eq. (2) is still valid. A monodisperse dilute polyelectrolyte with no added salt will contain only two ionic species. For one species, the polyion, a large molecule with a relatively small concentration c_p and a proportionally large charge Z_p, the equivalent conductivity λ_p is dependent on its size and conformation; thus

$$\sigma = Z_p c_p \lambda_p + z_i c_i \lambda_i . \tag{3}$$

Here we note that c_i is the concentration of counterions released from the polyelectrolyte upon solvation and is proportional to the concentration of monomers c constituting the polyion. The monomer concentration c is related to the polyion concentration c_p via

$$c = N c_p , \tag{4}$$

where N is the polyion degree of the polymerization. Also, the polyion charge is related to the monomer charge z_p:

$$Z_p = N z_p \tag{5}$$

due to the electroneutrality of the solution

$$Z_p c_p = z_i c_i = z_p c. \tag{6}$$

Thus the conductivity of a polyelectrolyte solution principally depends on the concentration of the monomers c:

$$\sigma = z_p c(\lambda_p + \lambda_i). \tag{7}$$

Here we remind readers that the polyion charge is effectively reduced, $Z_p = \theta N z_p$, due to the counterion condensation and also that only the free fraction θc_i of counterions is considered to take part in electrical transport. Therefore

$$\sigma = \theta z_p c(\lambda_p + \lambda_i). \tag{8}$$

The polyion conductivity λ_p, being defined by polyion mobility, actually stems from the self-diffusion coefficient of the polyion D_p and its charge Z_p, according to Einstein's relation for a charged particle:

$$D_p = \frac{kT\mu_p}{eZ_p} \tag{9}$$

and thus

$$\lambda_p = F Z_p e \frac{D_p}{kT}. \tag{10}$$

The diffusion coefficient depends on the size and shape of the particle, as well as on the viscosity of the solution in which the particle is moving. Inserting Eq. (10) into Eq. (8) we get

$$\sigma = \theta z_p c \left(F\theta N z_p e \frac{D_p}{kT} + \lambda_i \right). \tag{11}$$

Consequently, the conductivity of a monodisperse polyelectrolyte without added salt is primarily governed by the self-diffusion coefficient D_p of its polyion and the free counterion fraction θ.

In order to quantify the effects of the diffusion and electrostatics in a polyelectrolyte we used nucleosomal DNA fragments 150 bp (50 nm) long. These are expected to be rather rigid and rodlike since the DNA persistence length is 50 nm [27]. The dilute-semidilute crossover concentration for these fragments is ≈2 mM [28]. The details of material preparation and experimental methods are given in Sec. II. As presented in Sec. III, conductivity measurements were complemented by fluorescence correlation spectroscopy (FCS) measurements of the DNA polyion self-diffusion coefficient D_p. Our proposition, discussed in Sec. IV, is that the conductivity crossover observed in the $c = 0.05$–1 mM (in base pair) DNA concentration range results from the DNA denaturation that induces a concomitant change in the extent of Manning condensation. Eventually, we estimate the free counterions fraction θ and compare them with the values predicted by Manning for both ssDNA and dsDNA.

II. MATERIALS & METHODS

A. Monodisperse DNA

We will express DNA concentrations as molar concentrations of base pairs (bp) (1 g/L equals 1.5 mM bp). As above in Sec. I, c denotes concentration of monomers (here DNA base pairs) *i.e.* c is monomolar concentration.

Large quantities of practically monodisperse nucleosomal DNA fragments were prepared as described in Sikorav *et al.* [29] by enzymatic digestion of H1-depleted calf thymus chromatin [30]. This DNA, denoted DNA146, contains fragments 150 ± 10 bp long (50 nm) together with traces of 300–350 bp fragments that correspond to two nucleosomal DNA fragments connected by undigested linker DNA. DNA fragments were precipitated with cold ethanol, dried and stored at 4°C. The stock solution was prepared by dissolving 10 mg of the Na-DNA pellet in 0.55 mL pure water. A low-protein

content was verified by UV absorption. DNA146 solutions (0.015–8 mM bp) were prepared by dilution with pure water of aliquots from this 27 mM mother solution. To check that no salt was released from the pellet in addition to the Na^+counterions (2 Na^+ per bp), an aliquot of the pellet was dissolved in 10 mM NaCl, diluted five times with pure water and spin filtered to the original volume. This procedure was repeated three times. Another sample was simply dissolved in pure water. The two samples had similar conductivities (normalized for concentration). We concluded that any salt that may have been present in the pellet did not raise the conductivity more than the equivalent of 0.2 Na^+ ions per base pair.

110 bp dsDNA was prepared as follows. Two separate oligonucleotides (ssDNA, 110 nt) were purchased (Mycrosynth A.G., CH) [31]. The two sequences were complementary, and one of them was labeled at one end with a covalently bound Cy5 fluorophore. The dry complements were dissolved in 10 mM Tris-EDTA (TE) buffer with up to 60 mM NaCl, mixed and heated to 97 °C for 15 minutes to remove any hairpin loops previously formed, and then left to cool for several hours to slowly hybridize and form 110-bp-long dsDNA. Hybridization was checked to be complete on an agarose gel. To remove any NaCl excess, the solution was diluted four times with a large volume of 10 mM Tris-Cl buffer and then spin concentrated to the original volume. The procedure was repeated three times. In the resulting solution (denoted DNA110* with * to indicate the fluorescent labeling), the DNA and Cy5 concentrations were, respectively, 0.5 mM and 5 μM.

For FCS measurements, 2 μL of DNA110* stock was added into 500 μL DNA146 of varying concentrations (0.0015–8 mM concentration range) to achieve a 20 nM Cy5 concentration. Consequently, the 10 mM Tris of the DNA110* stock was diluted 250 times. Therefore, FCS measurements were performed on DNA solutions in the presence of very low added salt concentration ($c_{\rm salt} < 0.05$ mM). For FCS calibration, Cy5 fluorophore alone was diluted in pure water to 20 nM. Since the fluorophore concentration can deviate only less than one order of magnitude from this concentration, the amount of fluorescently labeled DNA110* was fixed, whereas the concentration of DNA146 spans several orders of magnitude.

B. Fluorescence correlation spectroscopy

Fluorescence correlation spectroscopy inherently probes the system under study both at single molecule and ensemble levels. FCS observes fluorescence intensity fluctuations emitted by fluorescently labeled objects diffusing through a small open volume (<1 fL) defined by the profile of the laser beam and the optics objective of the microsope. That is, the fluctuations in the number of the molecules entering and leaving the focal volume are registered as fluorescence variation, which is then recorded and autocorrelated. Thus following practically single molecules we obtain the properties of the ensemble [32,33]. We have used a commercially availabe Zeiss ConfoCor II FCS instrument, where the measurement volume was defined by a Zeiss Plan-NeoFluar 100×/NA1.3 water immersion objective, and epi-illumination was by He-Ne 632.8 nm 5 mW laser, for excitation of Cy5 fluorophore. Measurements were performed at 25°C, the ambient temperature of the temperature stabilized clean room. Zeiss proprietary software was used for the autocorrelation function calculation and extraction of diffusion times by nonlinear least-squares fitting [34]. The physical principles of such an experimental setup and theoretical background of FCS have been described elswhere [33,35]. The manner used to obtain the self-diffusion coefficient of the molecule under study, in our case 110 bp Cy5 labeled dsDNA, is presented in brief in the following. The instrument directly measures fluorescence intensity for, e.g., 30 seconds. The autocorrelation function $G(\tau_c)$ is calculated for the intensity trace, with the correlation time τ_c as the variable. The fluorescence intensity autocorrelation function $G(\tau_c)$ is fitted with a diffusion time τ. This FCS diffusion time relates to the characteristic time for fluorescent particle to diffuse through the focal volume. Autocorrelation function decays exponentially and is fitted to

$$G(\tau_c) = \frac{1}{N_f}\frac{1}{1+\frac{\tau_c}{\tau}}\frac{1}{\sqrt{\left[1+\left(\frac{w_0}{z_0}\right)^2\frac{\tau_c}{\tau}\right]}} \times\left[1+\frac{T}{1-T}\exp\left(-\frac{\tau_c}{\tau_T}\right)\right]. \quad (12)$$

Here N_f is average number of fluorescent molecules in the confocal detection volume. The transition of the Cy5 fluorophore to the first excited triplet state and a relatively slow relaxation to ground state influence the observed autocorrelation curve. Thus, T, the average fraction of fluorophores in the triplet state, and τ_T, the lifetime of the triplet state of the fluorophore, are taken into account when fitting. Another fit parameter is z_0/w_0, the structure parameter, i.e., the ratio of the axial and radial extension of the focal volume. The structure parameter $z_0/w_0 \approx 10$ is obtained from fits to autocorrelation curves measured for Cy5 molecules in pure water solution. Then it is kept as a fixed parameter when τ is later being extracted for DNA110*. The self-diffusion coefficient D_p of any particle is easily obtained from its FCS diffusion time τ as these are inversely proportional. Since the diffusion coefficient of Cy5 is known, $D_{\rm Cy5} = 3.16\times10^{-10}$ m^2/s [34], and the diffusion time $\tau_{\rm Cy5}$ was found to be about 50 μs, this provides means for conversion of the diffusion times τ into D_p:

$$D_p = D_{\rm Cy5}\frac{\tau_{\rm Cy5}}{\tau}. \quad (13)$$

C. Conductometry

Dielectric spectroscopy in the range 100 Hz–110 MHz was performed with the Agilent 4294A impedance analyzer. All the measurements were performed at 25°C. Conductometry data were extracted from these spectra. Conductivity was calculated from conductance at 100 kHz, and capacitance was read at 10 MHz. Conductivity at 100 kHz shows a minimal influence from the electrode polarization effects, as well as from the conductivity chamber resonance at 100 MHz. Basically, one has to measure a spectrum [36] to be able to confidently extract conductivity values. Only in this manner can the obtained conductivity be regarded as dc conductivity, the conductivity related to currents of freely mobile charges (polyions and

free counterions), and not due to polarization currents. We emphasize that all the conductivities of polyelectrolytes have been deducted for 1.5 μS/cm, the conductivity of the solvent [37], i.e., pure water (Milli-Q, Millipore). This residual conductivity is due to the ambient CO_2 dissolved in pure water. In this manner, pure water solutions may be regarded as very low added salt concentration solutions, $c_{\text{salt}} < 0.01$ mM, and we labeled them appropriately. The pH of pure water exposed to air is about 5.5; however, this is unbuffered. The capacitance at 10 MHz serves as a check of the sample volume for our experimental setup [38]. At this high frequency the contribution to the capacitance comes from the dielectric constant of pure water and not from the solutes. Thus all the samples should have the same capacitance if they have the same volume.

III. RESULTS

A. Electrical transport

We present the dc conductivity data of 0.015–8 mM DNA146 solutions. Experiments were performed at 25 °C in the absence of added salt (salt concentration $c_{\text{salt}} < 0.05$ mM) on the untreated DNA solution and after DNA denaturation. Figure 1(a) emphasizes a general power-law dependence of polyelectrolyte conductivity on monomer concentration [see Eq. (8)]. However, a slight S-shaped bending may be noted in $\sigma(c)$ for the untreated sample (black circles). After 20 min at 97 °C, followed by a quenching to 4 °C for 1 minute, the conductometry was performed at 25 °C. For these denatured samples (open circles) the power law is apparently better defined.

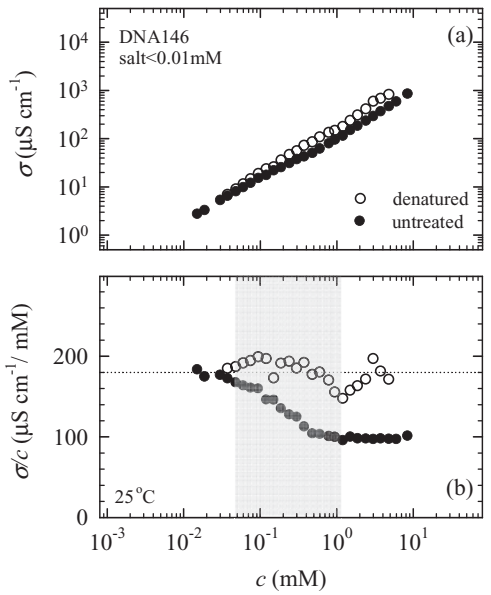

FIG. 1. Conductometry data for DNA146 solutions before (black circles) and after denaturation at 97 °C (open circles). (a) DNA146 solution conductivity versus DNA base pair (monomer) concentration. (b) Conductivity normalized by concentration versus DNA base pair (monomer) concentration. The dotted line shows the average value for denatured samples, 180 μS cm^{-1}/mM. The values for untreated samples at the lowest concentrations also approach this value. Shaded rectangle denotes the crossover concentration region. Measurements were performed at 25 °C.

If we normalize the conductivity with concentration, then data may be presented in a physically more relevant form [Fig. 1(b)]. That is, normalized conductivity concentration dependence is directly related to the behavior of the molar conductivities of Na^+ counterions $\lambda_i = \lambda_{Na^+}$ and DNA polyions λ_p:

$$\frac{\sigma}{c} = 2\theta(\lambda_{Na^+} + \lambda_p). \tag{14}$$

Here the factor 2 stands for DNA monomer charge (valence)$z_p = 2$ [see Eq. (8)]. We deem that the normalized conductivity (open circles) of the denatured samples is, within the data scatter, constant, with a value of 180 μS/cm. The data for denatured samples show a rather high scatter, which we ascribe to the denaturation procedure. Either denaturation did not proceed to the full extent for all the samples or some of the DNA renatured in hairpins during quenching [39], and this introduced a conductivity variation. Gradual renaturation, after quenching, and during the measurement at 25 °C was not an issue, as the samples held in our conductivity chamber showed a stable conductivity for at least an hour, and the measurement itself lasted for only 2 minutes.

Contrary to the denatured DNA, the normalized conductivity of the untreated DNA146 samples shows a crossover in the 0.05–1 mM concentration range (the crossover region is denoted by a shaded rectangle). Above 1 mM it attains a constant value of 100 μScm^{-1}/mM, while at the lowest concentration it approaches the 180 μScm^{-1}/mM value for the heat-treated, denatured DNA146 samples. This conductivity crossover has not, to our knowledge, been reported previously, for any DNA sample.

B. Polyion diffusion

We had to check whether the observed conductivity crossover relates to a change in DNA146 conformation due to DNA denaturation expected in the very low salt environment [40]. Therefore, we had to obtain the concentration dependence of the self-diffusion coefficient D_p for the DNA146 polyion for the concentration range studied by conductometry. However, the FCS diffusion times τ were measured for fluorescently labeled DNA110* polyion diffusing freely along the DNA146, but not for DNA146 itself. The labeled DNA is somewhat shorter than the bulk of DNA in the sample solution. Thus diffusion coefficients $D^{\text{exp}}_{110*}(c)$ for DNA110* that may be derived according to Eq. (13) had to be extrapolated to obtain $D^{\text{exp}}_{146}(c)$ values for DNA146. That is, DNA110* and DNA 146, 38, and 50 nm long, respectively, have lengths comparable to the dsDNA persistence length $L_p = 50$ nm [27]. Thus, an extended rodlike configuration might be expected, especially at low salt conditions. According to Tirado *et al.* [18] the translational diffusion coefficient calculated for a rodlike macromolecule is given by

$$D^{\text{th}} = \frac{kT}{3\pi\eta}\frac{\ln(L_c/d) + 0.312}{L_c}. \tag{15}$$

Here $L_c = Nb$ is contour length, d is polyion diameter, and η is viscosity of water ($T = 298$ K). Stellwagen *et al.* [19] have reviewed the literature and shown that the expression by

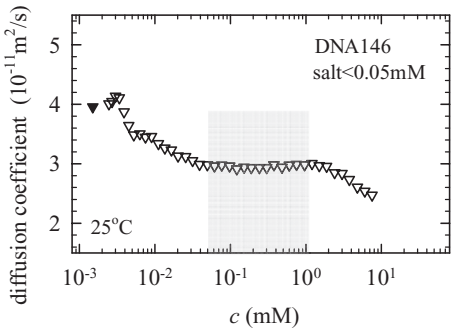

FIG. 2. Diffusion coefficient $D^{\mathrm{exp}}_{146}(c)$ for DNA146 polyion, obtained by fluorescence correlation spectroscopy (FCS) is shown versus DNA base pair (monomer) concentration c. Shaded rectangle denotes the crossover concentration region identified from conductivity measurements. Black triangle denotes diffusion coefficient D^{ss} derived for 146 bp ssDNA.

Tirado *et al*. is well applicable to experimental data obtained for DNA molecules in size from 10 to 1000 base pairs. Then, the relationship which holds between the theoretical values should also hold for the experimental values obtained at varying DNA146 concentrations c. Thus,

$$D^{\mathrm{exp}}_{146}(c) = \frac{D^{\mathrm{th}}_{146}}{D^{\mathrm{th}}_{110*}} D^{\mathrm{exp}}_{110*}(c). \tag{16}$$

Using Eq. (15) to get D^{th}_{146} and D^{th}_{110*} and Eq. (13) to get D^{exp}_{110*} from the diffusion times τ measured for DNA110*, we directly convert τ into D^{exp}_{146}. In this manner, fluorescence correlation spectroscopy provides the self-diffusion coefficient of DNA146 polyion, $D^{\mathrm{exp}}_{146}(c)$ at varying concentrations ($c =$ 0.0015–8 mM, base pair). The results are shown in Fig. 2.

First, we note that $D^{\mathrm{exp}}_{146}(c)$ is practically constant in the crossover concentration region $c = 0.05$–1 mM identified from conductivity measurements (denoted by a shaded rectangle). $D^{\mathrm{exp}}_{146}(c)$ starts to vary only above 1 mM. This coincides with the dilute-semidilute crossover concentration for 50-nm-long DNA146 molecules [28]. At higher concentrations the polyions start to overlap and the apparent viscosity of the solutions changes, inducing the decrease of the diffusion coefficient [41]. The fact that our probe DNA110* "feels" the phenomenon (the dilute-semidilute crossover) due to DNA146 demonstrates that DNA110* diffusion properties indeed reflect the DNA146 diffusion.

Second, below the crossover range $D^{\mathrm{exp}}_{146}(c)$ starts to increase toward the value D^{ss} (black triangle in Fig. 2) calculated, according to Eq. (13) and Eq. (16) from $\tau^{\mathrm{ss}}_{110*}$ obtained for the 110-bases-long ssDNA in pure water, without DNA146. This ssDNA is a sample of the Cy5 labeled synthetic oligonuclotide, dissolved in pure water, before any treatment (before mixing and hybridization with its complement). It is conceivable that D^{ss} is the limiting value for a series of decreasing DNA146 concentrations. That is, due to the very low added salt environment (practically without it: $c_{\mathrm{salt}} < 0.05$ mM) and the rather low DNA concentration and correspondingly low counterion concentration [40], we presume that DNA denatures below 0.05 mM and becomes ssDNA.

IV. DISCUSSION

Osmometry for dsDNA [9–11] has so far been the primary experimental source of θ data of sufficient quality to validate extensions to Manning theory [7]. Conductometry has been performed on different synthetic polymers, and has so far given results for θ that agree with Manning only within a prefactor of the order of unity and may depend strongly on the monomer concentration even in dilute solution [12,15–17,42]. We note that these experiments were performed either in semidilute solutions or with polydisperse samples, and, most importantly, the synthetic polymers used were usually rather flexible. We remind readers that in these cases the conformation of the polyion is not well defined and renders analysis difficult due to the necessity to introduce a model for the conformation, besides the model for condensation and conductivity. However, modeling conformation of a flexible polyion in a varying salt and monomer concentration is an elaborate problem in itself [14,26].

On the contrary, our DNA146 has a well-defined and simple rodlike conformation, and it is highly monodisperse and forms a dilute solution. DNA in the very low added salt (or in absence of salt) aqueous solution is also distinct as it is expected to go through melting transition with decreasing DNA concentration, so we could have ssDNA or dsDNA in solution, depending on the concentration [43]. That is, this may allow us to compare $\theta(c)$ results to Manning values for both ssDNA and dsDNA in one experiment. Actually, counterion condensation is related to the DNA stability: Entropic cost to condense or confine the counterions compares with the gain in electrostatic free energy upon DNA denaturation [3,44]. This gain is due to the single-stranded DNA (ssDNA) having a lower linear charge density parameter than dsDNA, $u = 1.7$ and 4.2, respectively. Accordingly, the free counterions fraction should be higher for ssDNA, $\theta = 0.59$, than for dsDNA, $\theta = 0.24$. We have shown in Sec. I how such an increase in θ would lead to an increase in the polyelectrolyte conductivity; see Eq. (11).

Most importantly, we have measured the self-diffusion coefficient $D_p(c) = D^{\mathrm{exp}}_{146}(c)$ of DNA146 as a function of DNA concentration. As we will show in the following, this allowed us to deconvolute the influence of DNA polyion charge, i.e., counterion condensation and the DNA polyion conformations on our conductometry data, which are a function of both. We start with DNA polyion molar conductivity, defined by

$$\lambda_p = F 2\theta N \mathrm{e} \frac{D_p}{kT}. \tag{17}$$

First, we note that this applies both for ssDNA and dsDNA. Comparing this expression with Eqs. (10) and (11), we find that for the valence we inserted $z_p = 2$. This is due to two negative charges (phosphate) being found on a single base pair in native dsDNA, which are still present on two separate nucleotides on two separated strands of ssDNA. Certainly, for an ssDNA of similar N as an dsDNA z_p equals one. However, since two ssDNA polyions appear in solution as a result of melting of one dsDNA molecule, the ssDNA concentration is doubled compared to dsDNA. This cancels the halved z_p, so there is no effect of melting on the polyelectrolyte conductivity σ, beyond the variation in θ or in D_p. Thus, for the sake of clarity, we

can proceed by keeping the factor 2 within λ_p, never mind the DNA state.

Inserting Eq. (17) into the expression for DNA conductivity [Eq. (14)] we get [see also Eq. (11)]

$$\frac{\sigma(c)}{c} = 2\theta\lambda_{\mathrm{Na}^+} + 4\theta^2 N D_p(c)\frac{Fe}{kT}. \tag{18}$$

This is a quadratic equation for $\theta(c)$ as a variable and $D_p(c)$ and $\sigma(c)$ as the parameters:

$$\theta(c)^2 + \frac{\lambda_{\mathrm{Na}^+}}{D_p(c)\times \text{const.}}\theta(c) - \frac{\sigma(c)}{c}\frac{1}{2D_p(c)\times \text{const.}} = 0. \tag{19}$$

Here const. stands for a product of several constants (defined previously): $2NFe/kT$. Our measurements of the DNA146 polyelectrolyte conductivity $\sigma(c)$ and our independent probe of DNA146 diffusion coefficient $D_p(c) = D_{146}^{\mathrm{exp}}$ (Figs. 1 and 2) allow for the equation to be solved for the free counterion fraction θ, without a necessity to model the DNA conformation. The equation is to be solved repeatedly for each concentration c, resulting in a concentration dependence $\theta(c)$. We take only the positive solutions as the physically meaningful.

The concentration dependence $\theta(c)$, according to Eq. (19), for DNA146 in pure water is shown (squares) in Fig. 3. At lower concentrations it reaches a value $\theta = 0.45$. Above 0.05 mM, in the conductivity crossover regime it starts to decrease, and above about 1 mM, outside crossover it becomes constant at $\theta = 0.30$. It is apparent that the experimentally derived range of values for θ falls within the theoretical Manning values for ssDNA and dsDNA, as denoted by dashed lines in Fig. 3. Also, it may be noted that the 50% variation in θ coincides with the conductivity crossover regime (denoted by the shaded rectangle). This is not surprising, as $\sigma(c)/c$ is the only variable parameter in Eq. (19), while the polyion diffusion coefficient D_p is rather constant in this regime.

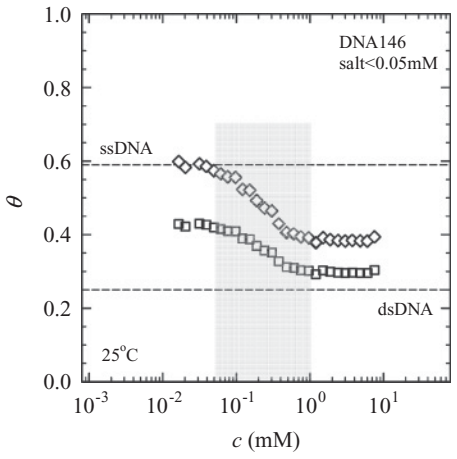

FIG. 3. Free counterion fraction θ for 146 bp nucleosomal DNA (DNA146) in pure water versus the DNA base pair (monomer) concentration c. Squares denote $\theta(c)$ calculated according to Eq. (19). Diamonds denote $\theta'(c)$, the results of a calculation where the assymetry field effect was taken into account, Eq. (23). Dashed lines denote the theoretical value of $\theta = 0.24$ for dsDNA and $\theta = 0.59$ for ssDNA, as labeled. Shaded rectangle denotes the crossover concentration region identified from conductivity measurements.

The preceding calculation did not take into account the *asymmetry field* effect, due to the distortion of the counterion atmosphere surrounding the polyion, occurring when the polyion is subjected to an external electric field [3,16,24]. The original work by Manning was reviewed and presented by Bordi *et al.* [12] in the form presented here. The asymmetry field effect can be taken [16] as if it corrects θ, which appears in expressions for conductivity, Eqs. (8) and (14), by a factor $B = 0.866$. The factor, calculated by Manning, originates in the difference in the diffusion coefficients of counterions in the limit of infinite dilution and in the presence of polyions. The asymmetry field also influences the effective observable molar conductivity λ_p of the polyion that figures in the above mentioned expressions. First, it corrects the effective polyion charge through the factor B:

$$\lambda_p' = 2\theta B N D_p' \frac{Fe}{kT}. \tag{20}$$

Second, the diffusion coefficient of the polyion is also corrected due to the asymmetry field:

$$D_p' = D_p \frac{1}{1 + \frac{ND_p}{D_{\mathrm{Na}^+}} 2\theta B \frac{1-B}{B}}. \tag{21}$$

Importantly, the diffusion coefficient of the polyion $D_p = D_{146}^{\mathrm{exp}}(c)$ we have experimentally obtained by FCS, without an electric field and thus without the asymmetry effect. Also, D_{Na^+} is the diffusion coefficient of free Na^+ ions in a simple, dilute electrolyte, 1.33×10^{-9} m^2/s. Combining the above, Eq. (14) becomes

$$\frac{\sigma}{c} = 2\theta B(\lambda_{\mathrm{Na}^+} + \lambda_p'). \tag{22}$$

Inserting Eqs. (20) and (21) into Eq. (22) we get another equation that may be used to obtain the free counterion fraction:

$$\frac{\sigma}{c\lambda_{\mathrm{Na}^+}} = 2\theta B\left(1 + 2\theta B \frac{ND_p}{D_{\mathrm{Na}^+}} \frac{1}{1 + \frac{ND_p}{D_{\mathrm{Na}^+}} \frac{1-B}{B} 2\theta B}\right). \tag{23}$$

In analogy with Eq. (19), we rewrite this into a quadratic equation:

$$M/Bx(c)^2 + \left(1 - AM\frac{1-B}{B}\right)x(c) - A = 0, \tag{24}$$

where M stands for $\frac{ND_p}{D_{\mathrm{Na}^+}}$ and A stands for $\frac{\sigma}{c\lambda_{\mathrm{Na}^+}}$. We remind readers that both M and A are obtained experimentally as functions of c, and that the equation was solved separately at each c value, to get $x(c)$ (we take only the positive, physical solution).

In Fig. 3 we show the asymmetry-field-corrected $\theta'(c) = x(c)/2B$ (diamonds). Overall behavior of $\theta'(c)$ is analogous to $\theta(c)$ behavior calculated with Eq. (19). The variation in $\theta(c)'$ also occurs within the conductivity crossover region (denoted by the shaded rectangle), and the relative change of θ' in the crossover region remains about 50%. However, the absolute values are different. At low concentrations

$\theta'(c) = 0.60$ reaches the theoretical value for ssDNA $\theta = 0.59$, while at high concentrations it decreases only to $\theta = 0.4$.

The crossover in conductivity that we have observed for DNA aqueous solutions with negligible, very low salt concentration is reflected as the crossover in $\theta(c)$ (or $\theta'(c)$), the Manning free counterion fraction. The exact θ values may depend on whether basic corrections to polyelectrolyte conductivity are taken into account. Notwithstanding the details of the conductivity model [17], we emphasize that the obtained extremal values for θ correspond to Manning model predictions for both ssDNA and dsDNA (denoted in Fig. 3 by dashed lines). This also corroborates the expected DNA melting across the studied DNA concentration range.

Notably, our result complements the unique result by Auer and Aleksandrowitz [9] obtained by osmometry for DNA solutions without added salt. These authors studied a somewhat higher DNA concentration range 2–10 mM. For dsDNA they obtained an osmotic coefficient $\phi_0 = 0.16$ that would correspond to $\theta = 0.32$, and for ssDNA they got $\phi_0 = 0.24$ corresponding to $\theta = 0.48$ for ssDNA. The relationship between θ and ϕ_0 is given by Manning [3,17]. We find that it is very significant that both osmometry and our technique find θ for ssDNA only 50% larger than for dsDNA, while Manning condensation theory predicts more than 100%! While the details of DNA conformations (e.g., coiling or formation of hairpins in ssDNA) might be in the origin of this discrepancy, the limitations of the Manning model should also be acknowledged; DNA is not a simple line charge.

The correspondence between the osmotic and transport measurements draws our final remark. That is, both techniques independently validate Manning's notion that counterions differentiate into two functionally separate populations. However, there is no *a priori* reason for these experiments to find similar fractions for these populations. The transport techniques measure the contribution to polyelectrolyte conductivity of the polyion whose charge is reduced due to the condensed counterions that move along, as well as the contribution of free counterions that move opposite to the polyion in the external electric field. Osmometry identifies as free the counterion fraction that contributes to the osmotic pressure of the solution, that is, those counterions that diffuse freely at distance from the polyion. However, as mentioned in Sec. I, the radial distribution of counterions is continuous, and, beyond the Manning model, in calculations based on Poisson-Boltzmann (PB) theory it is rather arbitrary to define any given distance from the polyion as the extent of the condensed counterions zone [5]. Specifically, a nonlinear PB model has been worked out for a system very similar to our experimental one, rodlike polyelectrolyte dilute solutions in the absence of added salt, and is based on defining the two (condensed and free) zones around the polyion [4]. Now, according to our experiments, the condensed counterions zone radius should be less arbitrary. That is, as our conductometry study detects a reduced DNA polyion charge due to condensation and as the diffusion results indicate a DNA polyion diameter of 2.6 nm, then this is also the condensed counterions zone diameter. The condensed counterions are to be found in the immediate vicinity of the polyion, as initially suggested by Manning, and the cylindrical condensed counterions zone depicted in Ref. [4] should be very thin.

V. SUMMARY AND CONCLUSION

In this work we have quantified the Manning free (uncondensed) counterions fraction θ for dilute aqueous solutions of rodlike polyions, 150 bp DNA fragments. In these solutions a practically negligible concentration of monovalent salt was present, $c_{\text{salt}} < 0.05$ mM. Thus we validated the Manning condensation and conductivity theories devised for dilute aqueous polyelectrolytes in the absence of added salt.

Our conductometry study revealed that the DNA solution molar conductivity normalized by DNA concentration attains an almost 100% higher value below 0.05 mM than above 1 mM (base pair). The results for solutions of ssDNA (actually, samples of thermally denatured dsDNA) lacked this conductivity crossover. Then we applied fluorescence correlation spectroscopy (FCS) to find that the diffusion coefficient of DNA polyion D_p is practically constant in the crossover region. Thus, we have shown that the origin for the conductivity crossover lies in the increase of the free charge fraction and decrease of the effective polyion charge, due to changes in Manning condensation, which we were able to quantify. Depending on if the Manning asymmetry field effect was taken into the conductivity model or not, we obtained the values within the ranges $\theta = 0.40$–0.60 or $\theta = 0.30$–0.45, respectively.

The conductivity crossover and θ variation are easily related to be due to DNA denaturation. However, the 50% variation in θ that we observe is smaller than what Manning condensation theory predicts as a difference between dsDNA and ssDNA (more than 100%). Nevertheless, a 50% difference in θ between ssDNA and dsDNA was also obtained in osmotic pressure studies by other authors. We also found it surprising that variations in DNA conformation due to denaturation appear to be of lesser influence on the polyion conductivity. The above two issues lead to the question of how the DNA conformations population changes with a decrease in DNA concentration in the very low added salt (practically, in the absence of salt) aqueous environment. This is the subject of our following paper [45].

Further application of FCS, with samples subjected to an external electric field (similar as that used for conductometry), could quantify the asymmetry field effect on the diffusion coefficient of the DNA146 polyion and reveal in detail to what extent the condensed counterions move with the polyion. Finally, combined conductometry and FCS studies of dilute monodisperse DNA in added salt solutions could extend the studies of θ and further complement the data obtained by osmometry.

ACKNOWLEDGMENT

We gratefully acknowledge A. S. Smith and R. Podgornik for illuminating discussions. T.V. is thankful to S. Kempter for her assistance in the laboratory. This work is based on the support from the Unity through Knowledge Fund, Croatia, under Grant 22/08. The work was in part funded by IntElBioMat ESF activity. The group at the Institut za fiziku works within Project No. 035-0000000-2836 of the Croatian Ministry of Science, Education, and Sports.

[1] M. Rubinstein and R. H. Colby, *Polymer Physics* (Oxford University Press, New York, 2003); J. R. C. van der Maarel, *Introduction to Biopolymer Physics* (World Scientific, Singapore, 2007).

[2] V. A. Bloomfield, D. M. Crothers, and I. Tinocco Jr., *Nucleic Acids* (University Science Books, Sausalito, 2000).

[3] G. S. Manning, J. Chem. Phys. **51**, 924 (1969); **51**, 934 (1969).

[4] A. Deshkovski, S. Obukhov, and M. Rubinstein, Phys. Rev. Lett. **86**, 2341 (2001).

[5] M. Le Bret and B. H. Zimm, Biopolymers **23**, 271 (1984); M. Deserno, Ph.D. thesis, Johannes Gutenberg-University of Mainz, 2000.

[6] D. Hinderberger, H. W. Spiess, and G. Jeschke, Europhys. Lett. **70**, 102 (2005).

[7] P. L. Hansen, R. Podgornik, and V. A. Parsegian, Phys. Rev. E **64**, 021907 (2001).

[8] D. Antypov and C. Holm, Phys. Rev. Lett. **96**, 088302 (2006); Macromol. Symp. **245–246**, 297 (2006).

[9] H. E. Auer and Z. Alexandrowicz, Biopolymers **8**, 1 (1969).

[10] E. Raspaud, M. da Conceicao, and F. Livolant, Phys. Rev. Lett. **84**, 2533 (2000).

[11] W. Essafi, F. Lafuma, D. Baigl, and C. E. Williams, Europhys. Lett. **71**, 938 (2005).

[12] F. Bordi, C. Cametti, and R. H. Colby, J. Phys. Condens. Matter **16**, R1423 (2004).

[13] S. Fischer, A. Naji, and R. R. Netz, Phys. Rev. Lett. **101**, 176103 (2008).

[14] F. Bordi, C. Cametti, and T. Gili, Phys. Rev. E **66**, 021803 (2002).

[15] D. Truzzolillo, F. Bordi, C. Cametti, and S. Sennato, Phys. Rev. E **79**, 011804 (2009).

[16] C. Wandrey, Langmuir **15**, 4069 (1999).

[17] C. Wandrey, D. Hunkeler, U. Wendler, and W. Jaeger, Macromol. **33**, 7136 (2000).

[18] M. Mercedes Tirado, C. Lopez Martinez, and J. Garcia de la Torre, J. Chem. Phys. **81**, 2047 (1984).

[19] E. Stellwagen, Y. Lu, and N. C. Stellwagen, Biochemistry **42**, 11745 (2003).

[20] M. Mandelkern, J. G. Elias, D. Eden, and D. M. Crothers, J. Mol. Biol. **152**, 153 (1981).

[21] R. Pecora, Macromol. Symp. **229**, 18 (2005).

[22] A. Wilk, J. Gapinski, A. Patkowski, and R. Pecora, J. Chem. Phys. **121**, 10794 (2004).

[23] S. T. Hess, S. Huang, A. A. Heikal, and W. W. Webb, Biochemistry **41**, 697 (2002).

[24] G. S. Manning, J. Phys. Chem. **85**, 1506 (1981).

[25] G. S. Manning, J. Phys. Chem. **79**, 262 (1975).

[26] A. V. Dobrynin and M. Rubinstein, Prog. Polym. Sci. **30**, 1049 (2005); A. V. Dobrynin, R. H. Colby, and M. Rubinstein, Macromolecules **28**, 1859 (1995).

[27] C. G. Baumann, S. B. Smith, V. A. Bloomfield, and C. Bustamante, Proc. Natl. Acad. Sci. USA **94**, 6185 (1997).

[28] P. G. de Gennes, P. Pincus, R. M. Velasco, and F. Brochard, J. Phys. (Paris) **37**, 1461 (1976).

[29] J. L. Sikorav, J. Pelta, and F. Livolant, Biophys. J. **67**, 1387 (1994).

[30] T. E. Strzelecka and R. L. Rill, J. Am. Chem. Soc. **109**, 4513 (1987).

[31] Custom oligonucleotides 110 bases long, with complementary sequences as specified. Synthesis scale was 0.2 μmol with PAGE purification step. Cy5 fluorophore was covalently bound to 5′ end of sequence 2. Sequence 1 (5′–3′): GAA GGA GCG GCC AGA GAT TTC TCT TCC TTC AGA TTT TGA GCA TAC AAT TCA TGT TGG TTT TGA TGC TGT CAC AGG GGA GTT TAC GGG GAT GCC AGA ACA GTG GGC CCG CT; sequence 2 (5′–3′): AGC GGG CCC ACT GTT CTG GCA TCC CCG TAA ACT CCC CTG TGA CAG CAT CAA AAC CAA CAT GAA TTG TAT GCT CAA AAT CTG AAG GAA GAG AAA TCT CTG GCC GCT CCT TC.

[32] R. Rigler, Ü. Mets, J. Widengren, and P. Kask, Eur. Biophys. J. **22**, 169 (1993).

[33] P. Schwille, J. Bieschke, and F. Oehlenschlager, Biophys. Chem. **66**, 211 (1997).

[34] Carl Zeiss, *Applications Manual LSM 510 – ConfoCor 2* (Carl Zeiss, Jena, 2001).

[35] S. Mangenot, S. Keller, and J. Räedler, Biophys. J. **85**, 1817 (2003).

[36] S. Tomić, S. Dolanski Babić, T. Ivek, T. Vuletić, S. Krča, F. Livolant, and R. Podgornik, Europhys. Lett. **81**, 68003 (2008).

[37] S. Tomić, S. Dolanski Babić, T. Vuletić, S. Krča, D. Ivanković, L. Griparić, and R. Podgornik, Phys. Rev. E **75**, 021905 (2007).

[38] T. Vuletić, S. Dolanski Babić, T. Ivek, D. Grgičin, S. Tomić, and R. Podgornik, Phys. Rev. E **82**, 011922 (2010).

[39] A. Montrichok, G. Gruner, and G. Zocchi, Europhys. Lett. **62**, 452 (2003).

[40] M. T. Record Jr., Biopolymers **14**, 2137 (1975).

[41] M. P. B. Van Bruggen, H. N. W. Lekkerkerker, and J. K. G. Dhont, Phys. Rev. E **56**, 4394 (1997).

[42] F. Bordi, C. Cametti, A. Motta, and G. Paradossi, J. Phys. Chem. B **103**, 5092 (1999).

[43] W. F. Dove and N. Davidson, J. Mol. Biol. **5**, 467 (1962); M. T. Record Jr., Biopolymers **14**, 2137 (1975).

[44] G. S. Manning, Biopolymers **11**, 937 (1972).

[45] T. Vuletić, S. Dolanski Babić, T. Ban, J. Rädler, F. Livolant, and S. Tomić, Phys. Rev. E. (to be published).